



Preliminary Evidence for the Tectonic Influence on the Emplacement of the Gwandara Pluton in the Northcentral Nigeria Basement Complex

Peter Agbo^{1*}, Nathaniel Goker²

¹Federal Ministry of Environment, Abuja, Nigeria

²Department of Geology and Mining, Nasarawa State University, Keffi, Nigeria

Article history

Received 13 November 2025

Accepted 25 December 2025

Published 31 December 2025

Contact

*Peter Agbo

agbopeter@yahoo.com (PA)

How cite

Agbo, P., Goker, N.G., 2025. Preliminary Evidence for the Tectonic Influence on the Emplacement of the Gwandara Pluton in the Northcentral Nigeria Basement Complex. International Journal of Earth Sciences Knowledge and Applications 7 (3), 364–375. <https://doi.org/10.5281/zenodo.1807699>.

Abstract

This study presents the nature and pattern of field and microtectonic fabrics engraved in the Gwandara pluton as it relates to its emplacement around the southwest of Keffi, in the Northcentral block of the Nigerian basement complex. The granite pluton is part of the numerous isolated hills around Keffi, upstretched amidst polydeformed gneissic and schistose rocks. The pluton is characterized by patches of granodioritic materials and overlapped by a thermally healed fractural system that shows a hopscotch joint pattern with a sinistral strike-slip displacement pattern. Around the host rock, the deformation shows drag-stretching of early injected leucosome, development of ptygmatic folds, and realignment of veins that were supposedly perpendicular to the pluton. The strain estimate shows a strain partitioning pattern that is relatively homogeneous, defined largely by the mineral grain distribution. Anisotropy of Magnetic Susceptibility data suggests a dominantly NE-SW directional magmatism under transient tectonic conditions typical of a transtensional zone. Mineral quartz and feldspars show mechanical deformation and define the field lone-phased ductility that somewhat formed about the crystallization temperature of feldspars during an active regional deformation. Most of the structures resulted from the combined effects of phase transpose under a protracted deformation episode and magmatic stress field generated during pluton growth.

Keywords

Pan African tectonics, tectonic, influence basement complex, granite, deformation microstructures

1. Introduction

The Northcentral Nigerian basement complex is a cluster of reworked Archean-late Proterozoic rocks located around Central Nigeria. It is a section of the Nigerian basement complex that has been significantly deformed and warped by multiple trans-Atlantic structures and subsequent deposition of Cretaceous sediments. It is a fragment of the southern margin of the Neoproterozoic Trans-Saharan belt, generally referred to as the Nigerian Basement Complex, whose formation is largely based on terranes amalgamation and collision (Black et al., 1994; Caby, 1989; Ajibade et al., 1987; Ferré et al., 2002). The complex is characterized by high-grade metamorphic facies and pervasive structures that later controlled the most prolonged magmatic events in recent

geological history. This magmatism is responsible for the emplacement of the older granite series- a group of rocks that changes the architecture of the premodern topography. They are the most conspicuous magmatic component of the complex and occur as built-in hills rising steeply amidst polydeformed rocks of the migmatitic-gneisses and schistose complex (Pidgeon et al., 1976; Van Breemen et al., 1977; Dada et al., 1989; Dada et al., 1993).

The older granites were derived as products of composite contamination of mantle melt with older crustal melts in an assimilative relationship during the geodynamic episode that accompanied the Pan-African tectonics (Dada et al., 1995; Caby, 1989). Thus, the rocks appeared to be the major source



of crustal addition at the close of the Proterozoic period. Most of the plutons are calc-alkaline and are molded mostly by I-type magmatism and range in compositions between tonalite, granodiorite, granite, syenite, and charnockite (Trustwell and Cope, 1963; Egbuniwe et al., 1983; Haruna, 2014; Goki and Abba, 2019). Generally, the rocks occupy a large fraction of the complex in space and hold great cumulative historical clues on the nature of tectono-magmatic and crustal deformation.

2. Geology of the Study Area

The study area comprises composite lithological outcrops

typical of the Nigerian Basement Complex (NBC) rocks; undoubtedly related largely by prehistoric geomorphological dynamics and tectono-deformational history. Most of these relationships were driven by collative effects of multiple tectonics that defined the evolution of the complex. Phyllitic schist, migmatized gneisses, granitic gneiss, and the granitic series are the major lithologies in the study area (Fig. 1). The configuration of these rocks is a testament to the region's geological complexity and dynamics associated with multiple tectonothermal events shaping the lithological assemblage. Detailed litho-distribution of the study area has been reported by Agbo et al. (2025).

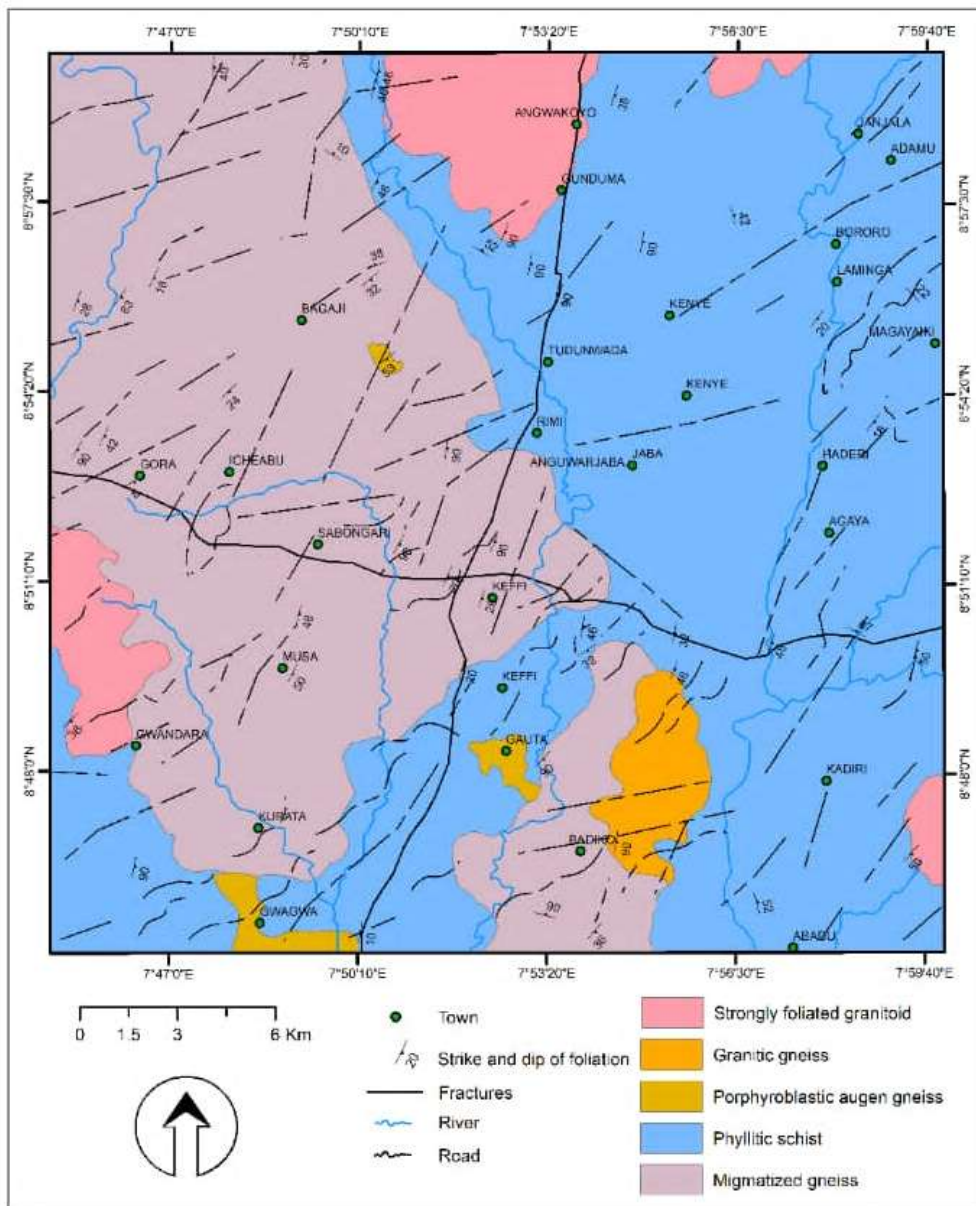


Fig. 1. Simplified lithostructural map of the study area (Agbo et al., 2025)

2.1. Structural-Magmatism

Field relationships show successive and cyclical magmatic activities whose influence affected the geomorphological processes that shaped the general geology of the study area. These events occurred around the same tectonic cycle, but the earliest phase coincided largely with a predominant

NNW-SSE to N-S structural system that later became circuits for hydrothermal crystallization. This process saw the birth of the protholith of the orthogneiss referred to as porphyroblastic and granitic gneisses, under a deformational regime accompanied by amphibolite facies metamorphism (Ugwuonah, et al., 2017).

Despite being deformed significantly by the later events, these rocks still retained relics of their magmatism, particularly the acquired xenoliths. The later phase of the magmatic activities coincided with the close stages of the tectonic activity. This stage was characterized by a total shift from an earlier structural system to a largely imperious NE–SW structural trend. These structures severely obliterated the earlier footprints, making it difficult to distinguish in relative terms the structural fabrics older than the event. Interestingly, this structural interaction with the older structure created transfer zones that contributed to the development of the spaces, as well as ascent paths and enacted control in the emplacement of the Pluton.

2.2. Litho-Metamorphism

The metamorphism as observed in the area was driven by crustal dynamics resulting from oscillatory T-P conditions associated with the tectonomagmatic activities. It is of the

amphibolite facies with a peak P-T condition of between 570 °C and 630 °C, and 6.4 - 7.7 kbar (Ugwuonah and Obiora, 2011; Ugwuonah et al., 2017).

Similar conditions have been reported across many Pan-African domains (Rahaman, 1988) and were collaborative in timing with the ductile deformational phase in the study area. The metamorphism has a regional homogeneity but generally grades around the pluton, and inhabited nuclei where effects were significantly felt. These areas are particularly around zones of high-temperature fluid interface, and constricted zones associated with shearing. This is evident in the recrystallization of quartzofeldspathic minerals in some lithologies, including the granitoids, the formation of minerals like the spotted staurolite found in phyllitic schist, reorientation of mineral lineation and foliation plains, and the development of myrmekitic intergrowths even at microscopic observations (Barker, 1998).



Fig. 2. a) Field evidences of compressive assimilation of the host rock by the magma, b) Field evidence of sinking block (pendent) of host rock into the magma chamber, c) Field evidences of compressive assimilation of the host rock by the magma and d) field evidence of near boudin which acted as heat loss circuit on the pendent

2.3. Structural and Deformational Pattern

Three major deformational episodes are recorded in the area and are mostly defined by foliation streaks and fractural systems. These are clustered into clusters corresponding to NE-SW, NW-SE, N-S, and a ghostly superimposed E-W. Each of the clusters perhaps did not develop independently of others, but the contrasted patterns show the intertwining complexity of the tectonic impacts and the multidimensional responses of the crust. The NW-SE cluster has a dominant streak in the southern portion of the study area, and it is considered the leftover of an earlier deformation herein considered as D1.

The foliations in this area are defined by the development of metamorphic fabrics generated by mineral growth and transposition of stratigraphic fabrics. The relationship between the two sets is discordant, suggesting deformation fabrics that are sequential in history. Foliation extends in intensity from a mere to a well-developed schistosity among schist to banding in the gneisses and development of gneissoid structures in some components of the granitic rocks. It has a lower proportion and corresponds largely with trends of mineralized pegmatite. They are cut and twisted in many locations where the NE-SW cluster shows great dominance. This cluster predates the NE-SW trends and

contributed to the development of planes of weakness in the basement complex. This is regarded as S1, and it reveals a bulk directional deformation pattern, particularly on phyllitic schist.

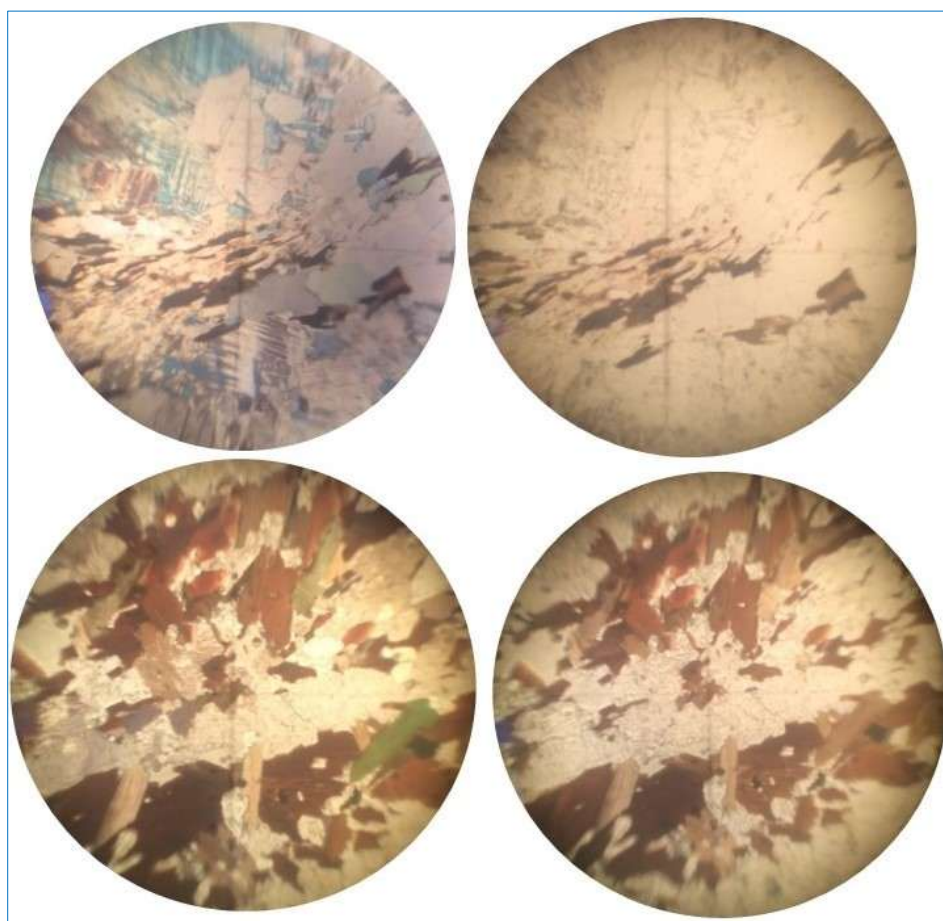
3. The Pluton

The pluton hereafter referred to as the Gwandara pluton is located in Gwandara village, SW of Keffi Sheet 208NE. The pluton is a massive laccolithic-shaped outcrop whose long axis is relatively oriented in the NE–SW direction. Its total outward length is estimated to be about 2km with an average width of about 500m. The outcrop can be described as a “core of phyllite and a casing of granite” because of its show of fractional assimilation of the host rock. The pluton is bounded to the west by ductile deformed phyllitic schist, and the immediate eastern vicinity of the pluton is conjoined by conjugate offshoots that show great resemblances in grain size distribution, mineralogy, and structural characteristics, suggesting a comparable parental development.

Compositionally, the rock is a biotite granite with patches of granodioritic composition, meddled by aplitic,

quartzofeldspathic, minor quartz, and mafic veins. It has quartz, feldspar, and micas as the major mineral constituents, while hornblende, chlorite, and epidote form parts of the minor components. The rock is relatively deformed with dominant lineation around portions associated with localized minor shear and fracture zones. There is an obvious crystal grain grading from coarsely porphyritic around the lower region to finely grained mostly around the uppermost region of the pluton, suggesting a likely sudden change in crustal conditions upward along the magma chamber.

Similarly, grain size fluctuations were recorded on the offshoots but developed within the boundaries of the in-between-grain boundaries defined mostly by structurally disposed aplitic and quartzofeldspathic veins. The lower part of the outcrop is predominantly porphyritic with individual porphyry ranges, averagely about 2 cm in diameter. At some locations, the porphyries constitute a significant portion of feldspathic veinlets that consecutively parallel the wall of the pluton. This scenario likely occurred at the pluton sub-solidus stage of crystallization, where the porphyries were already formed.



The western portion of the pluton is characterized by significant interactions between the enveloping magma and the host rock, as shown in the preserved massive xenoliths of highly baked host rock. The scenario is largely an overriding flown-over event that is evident in the granitic magma blanketing pattern over the host rock (Figs. 2a and 2c). The southern edge of the pluton holds a massive pendent of

phyllitic schist tilted with a probability of sinking into the pluton should the process continue beyond that stage. Interestingly, the adjoining base is significantly characterized by typical porphyritic textures associated with other locations - this depicted a host rock and ascending magma relationship that was compressively assimilative (Fig. 2b). The pendent was pervaded by rising hydrothermal fluid from the

ascending magma along pervasive cleavages, which resulted from the remote response of the sinking slab to energized magmatic forces; this resulted in considerable development of near-boudins of stretched quartz veins (Fig. 2d). The cleavages served as conduits for heat loss, which controlled the crystallization at the upper part of the pluton.

3.1. Micromorphology of Major Mineral Grains

Three major granite minerals (quartz, feldspar, and mica) were studied under a petrographic microscope to examine their reaction to deformation. Quartz is important because of its abundance amidst the mineral matrix of the rock; it has significantly controlled the bulk deformation pattern, because of its weak nature and reaction pattern to changes in temperature conditions as low as 150°C (Handy, 1990).

Quartz revealed dual paternity, defined as primary quartz, which resulted from the growth of individual crystals out of melt during magmatic crystallization, and secondary quartz resulted from near solid-state crystallization.

The secondary quartz is mostly found along microcracks and mylonitic foliation (Fig. 3) with less or no display of undulate extinction, unlike the earlier-formed grains that show evidence for brittle deformation. It has moderate to large-sized crystal grains with forms ranging from subhedral to anhedral. It shows perthitic intergrowth and occurs as an inclusion among many minerals, particularly feldspars. Quartz experienced only solid-state deformation, as opposed to the duo (including sub-magmatic) deformation common with feldspars.

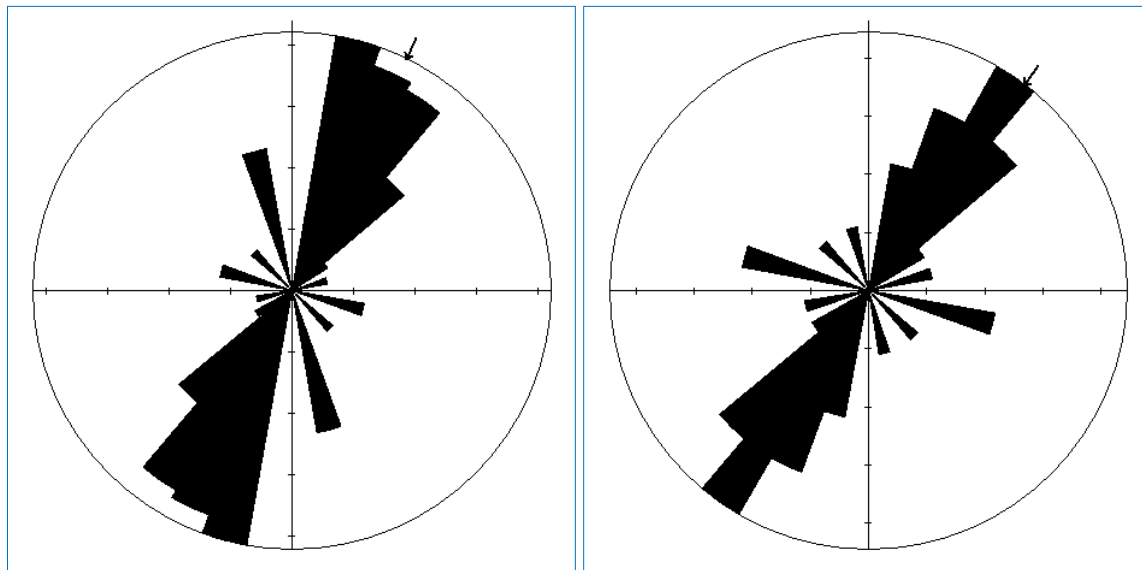


Fig. 4. Rosette plots for strike and dips trends on the pluton: a) Vertical fractures and b) Dipping fractures



Fig. 5. Healed fractures on the pluton

Unlike quartz, feldspar and micas also constitute a significant proportion of the mineral composition. These minerals not only provide a mirror image of the general outward ductility of the rock, but feldspar-dominated porphyries constitute the strain marker used for strain analysis. Feldspars show

pervasive intergranular brittle deformation in the pluton and constitute an aggregate of minerals deformed along the micro-mylonitic foliation zones as viewed under thin sections. It constitutes the bulk of the porphyritic property of the rock and contributes to the degree of lineation in the rock.

It is dominated by microcline and little andesine of the plagioclase, with little evidence of epidotization around some well-developed microphenocrysts.

Microcline is characterized by distinctive plaid twining, giving a zebra stripe appearance with a wavy extinction across some samples. It is generally between subhedral, anhedral, and sometimes cloudy. Similarly, micas constitute about 10 - 15% of the modal composition of the granites. Biotite appears to have more than 80% dominance but appears as long, skinny flakes largely stretched or crushed into a rumble, particularly along micro-deformation zones; this is indicative of strain conditions. They developed and constituted the dominant minerals indicated in the magmatic

foliation found in the granitoids. They enclosed muscovite along the micro-band, which indicates simultaneous crystallization of the minerals as shown in its intergrowth with hornblende. Biotite seems to overlay quartz and feldspars in many places and shows near-parallel extinction and well-developed cleavages.

Muscovite forms prismatic subhedral crystals deformed along the magmatic foliation. Muscovite seems not to be pleochroic, even though it sometimes shows a distant greenish-stained color. Other minerals like hornblende and chlorite are the minor minerals viewed in some samples; however, their statistical value limits their application in this evaluation.



Fig. 6. Evidence of field ductility on the rocks around Gwandara pluton: a-b) Transient shearing on the pluton and phyllitic schist, c) Sinistral strike-slip north of the pluton and d) Belts of constrict porphyries on the pluton

3.2. Pluton-Induced Deformations on the Host Rock

Generally, the contact between the pluton and the host rocks is largely impeded by plurimetric boulders; thus, where accessible, the host rock is significantly deformed and migmatized with a trait of forceful events. Most of the observations were made on the western flank of the pluton, as there is a total submersion of the host rocks to the east, as the crystallization of the offshoots literally obliterated the rock in a region of hundreds of meters away from the pluton, with only patches of compressed xenoliths sighted between two minor offshoots. The following were observed.

- i. There was significant evidence of lateral increase in the thermodynamic state along the contact at a temperature high enough to initiate depletion of muscovite up to about 100m into the phyllitic schist.
- ii. Development of a single-phase progressive deformation that resulted in the formation of minor isoclinal folds

whose coaxial planes are parallel to the pluton. This shows indications of a mild push-apart scenario that resulted from further space development for raising magma. Also, within the contact, there are cases of drag-stretching of early injected leucosome, development of ptygmatic folds, and realignment of veins that were supposedly perpendicular to the Pluton.

- iii. Lineation in the host rock is defined by the direction of stretched boudins and stretched foliation planes.
- iv. The preservation of a massive xenolith and dipping pendant is evidence of magmatic assimilation of the host rock.
- v. The long axis of the pluton corresponds with the regional NE-SW foliation planes recorded in the host rock.

The above observations show the implication of deformation on the host rock that is apparently contemporaneous with the emplacement of the pluton. Also, it shows that the host rock

was under an intense regionally ductile deformation that further weakened the transtensionally deformed crust, whose effects persisted until after the emplacement.

4. Macro Deformation Pattern on the Pluton

4.1. Brittle deformation

The pluton harbors considerable proportions of intertwined joint systems in association with significant faults of dislocated architecture. These fracture surfaces seemingly resulted from a singular but protracted stress regime that at intervals resonated in response to constrained active regional deformation, uneven cooling pattern, and magma-generated stress field during active emplacement episode where further expansion of the magma chamber was inevitable.

Also, recovering attempts of the Pluton under passive stresses might not be inconsequential. The cumulative effects of this scenario reverted some joints further into faults as evident in

the kinetic morphology revealed at most fault lines. This also accounts for the development of minor shear zones on the outcrop. The joints are predominant around the lower region of the major outcrop and the associated offshoot. The identified joint trends are consistently in the NE- SW, NW- SE, and N-S directions (Fig. 4); these trends may not have been formed independent of each other under multidimensional single brittle phase deformations.

The joints are mostly healed by aplitic materials in continuously slim linear to curvilinear surfaces and occur in groups of closely packed hopscotch. The faults group shows records of considerable displacement ranging in centimeters to meters in some locations and are typified by sinistral strike-slip faults (Fig. 5). This structural relationship occurred across lithologies but was conspicuous on the pluton. They are mostly healed by remnant fluids trapped within the cooling rock.

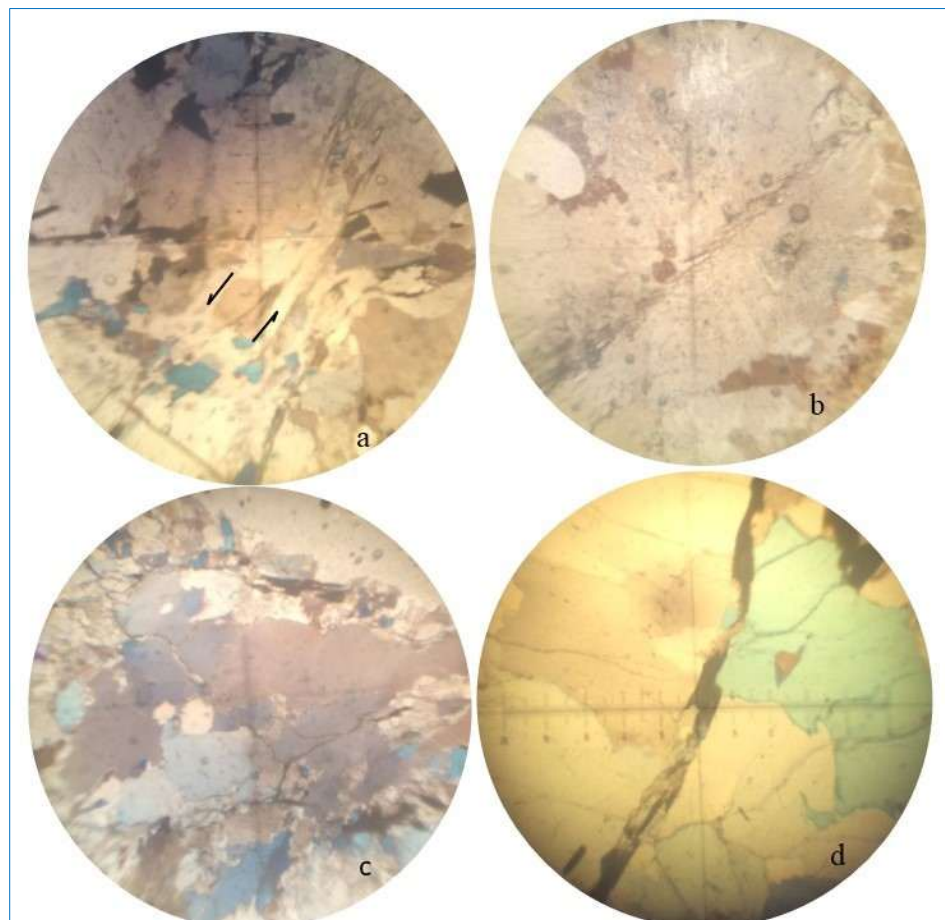


Fig. 7. Microstructures recorded in the Gwandara pluton: a) Mylonitic foliation with associated microfault, b) Cohesive fracture and c-d) Microcracks and banding

4.2. Ductile Deformation

The pluton showcases a NE-SW lone-phased lineation trend defined by a stretched boudins line, elongated mineral grains, aligned phenocrysts, magmatic enclaves, and xenolith (Fig. 6). This trend corresponds to the regional foliation planes recorded on both phyllitic schist and migmatized gneisses. Feldspar appeared the most lineated mineral grain in this rock. This perhaps suggests that the ductility of the rock was

largely recorded just around the crystallization temperature of feldspars such that the feldspar-rich porphyries became stretched. Most of the affected physical constituents of the rock that defined the monophased event share an orientation that dominantly fluctuates between 012° and 064° even though pockets of SE and SW trends were sighted. This lineation pattern is reflective of a viscous state of magma emplaced in the relative closing stages of an applied regional

stress field sequel to total solidification. The pockets of minor trends registered are largely due to some chamber-magma dynamics.

The superficial geometry of the porphyries plunges between 10° and 40° but dominantly around 20° which tallied with the two-stage vertical reverse faulting caused plunges reported on the NE-SW trending Maloney Hills (Goki and Ubugadu, 2022). Also, structural study of the area did not show regional extent shear zone except for minor zones of heterogeneous strain accumulation and some pockets of pulverized minerals crystal zones that are most likely mylonitised (Fig. 6a). These structures are also commonly recorded on the phyllitic schist (Fig. 6b). Those of the plutons are largely attributed to solid-state deformations that are typical of temperatures below 500°C (Gapais, 1989).

5. Microstructures in the Pluton

The microstructure morphology of these rocks is characterized by various degrees of microcracks, joints, and associated microfaults (Fig. 7). These range between those healed by quartz and/or feldspar minerals constituents typical of submagmatic conditions, and those dried and predominantly associated with quartz and feldspars typical of solid-state deformations. The microcracks are mostly intragranular and pervasive with dissimilar microtrends, although those common on feldspars show concentration in the NE-SW directions. The micro faults and joints are

intergranular with mostly NE-SW plane trends typified by sinistral strike-slip and cohesive breccia fault system. They are formed during transient strains generated by grain-boundary friction in a solid stage of the pluton at uneven temperatures fluctuating around feldspar crystallization temperatures. The microfractures obviously show formation at temperatures that are likely lower than quartz crystallization temperatures, where the pluton has exhausted the remnant-held magmatic fluid before total quartz crystallization. Microfoliation, the ductility recorded in the rock, is characterized by two sets of microfoliation planes as viewed under the petrographic microscope. This set occurs in bands and is categorized as *Magmatic* and *Mylonitic foliation* planes. Both share similarities in trends and patterns, with consistent trends predominantly in the NE-SW direction.

The *Magmatic Foliation* is defined by two bands of segregated platy minerals of mostly biotite, representing the dark band and felsic band, predominantly quartz. These bands are characterized by an undergrowth of pure quartz, and in some places, flow created voids to overlap biotite. This quartz set may not be associated with further injection of magmatic pulse but represents the remobilized leftover fluids trapped within already crystallizing minerals which is largely influenced by mineral kinesis induced by regionally applied stress field. This scenario is typical of a submagmatic state phenomenon characterized by increased pressure conditions on an embryonic pluton.

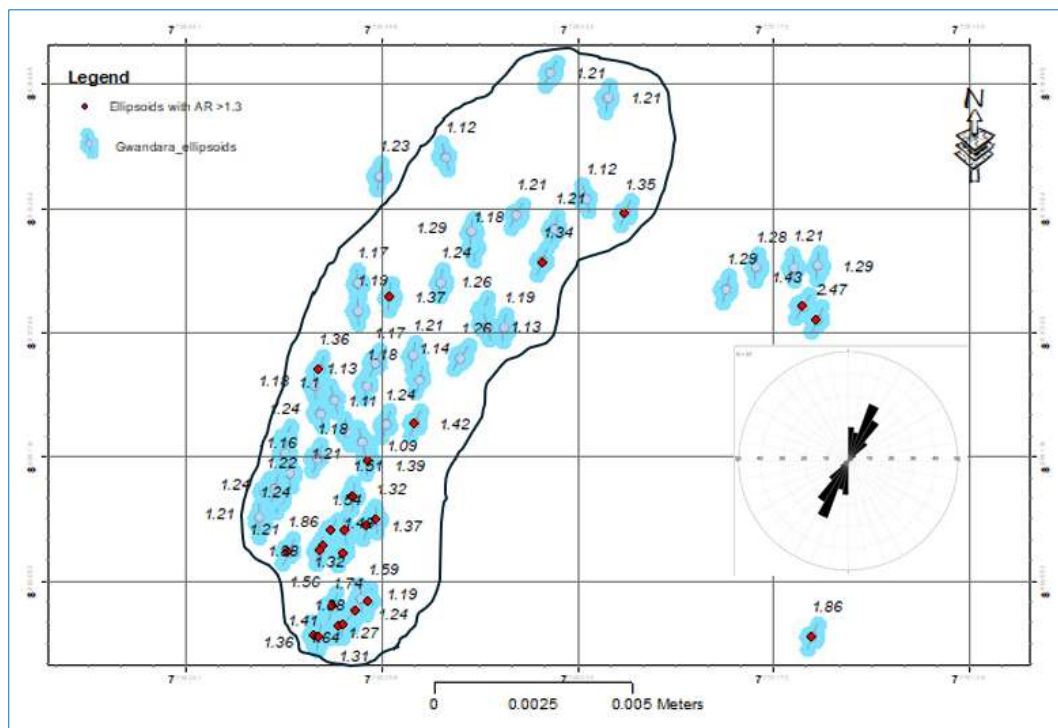


Fig. 8. Distribution pattern of strain ellipsoids trends on Gwandara pluton

The *mylonitic foliation* planes are defined primarily by a collection of crumpled and remobilized minerals in the neighborhood of two stable mineral grains. Biotite conspicuously shows flowage while quartz remains relatively undeformed. Dusts of realigned feldspar were seen across the

plane, while chunks of crumbled feldspar were sinistrally displaced (Fig. 7a). This is a constricted strain zone that largely seems to be a phase-lift or transposition of the earlier formed magmatic foliation at a further increased pressure. The relationship between these planes shows that there was

a protracted increase in pressure (with a decrease in temperature) conditions along a strait throughout the crystallization history of the pluton.

6. Strain Distribution

Strain estimates on these outcrops were carried out with the target of providing bases for a critical understanding of the emplacement kinematics. In this study, two sets of data were used: the phenocrysts on the granitic rocks and the thin-section micrographs. The phenocrysts were considered good markers, having exhibited homogeneity in kinetic characteristics typical of a flow lineation. On the other hand, thin-section micrographs were used for another set of rocks, i.e., rocks devoid of phenocrysts. Both photographic samples were serenely digitized by marking the center of the entire grains on the selected micrographs of the rocks using the GeoFry application, and the result is a Fry hollow of ellipsoidal shapes presenting the long and short axes. The phenocryst is important because it constitutes an integral component of the rocks and apparently the most conspicuously deformed mineralogical pieces.

Seventy-nine (79) field photos of phenocrysts were sampled and plotted across the plutons. The resultant axial ratio ranges between nearly circular (1.09), which is indicative of the low degree of deformation and thus less strained mineral grains, while the nearly stretched ellipsoids correspond to regions with a relatively higher axial ratio (2.47). The shapes of the ellipsoids generated show varied orientations but trends predominantly in the NE-SW directions and marginally in the NW-SE trends, which coincidentally are the trends of most deformational signatures in the study area (Fig. 8). Evaluation indicates strain constrictions decrease progressively around the contact corridor into the pluton and along with its vertical extent. Though the variation does not differ significantly across lithology, the show of a decrease in the strain upward is tied to an intense reduction in grain sizes.

This variation is also evidenced in the foliation pattern recorded on the phyllitic schist and the deflection in some

minor dykes, i.e., where strain is lessened, these veinlets displaced stability; therefore, strain is limited by distance away from the circumference of the pluton.

7. Anisotropy of Magnetic Susceptibility

The Anisotropy of Magnetic Susceptibility (AMS) is a critical aspect of this study due to its effectiveness in evaluating deformation in weakly deformed rocks and/or in rocks where deformation cannot be physically measured (Tarling and Hrouda, 1993; Borradaile and Henry, 1997; Evans et al., 2003). AMS is employed in this study because the pluton is relatively undeformed, except where lineation fabric is obvious. The results include micromagnetic parameters that have significant geological implications and provide useful insights into the deformational patterns recorded in the rocks.

The parameters considered for this study include Magnetic mean susceptibility (K_m) = $(K_1 + K_2 + K_3)/3$. K_m measures the average magnetic response of each sample. Other parameters include anisotropy ratios $L = K_1/K_2$ (Lineation) $F = K_2/K_3$ (Foliation) $P = K_1/K_3$ (Degree of anisotropy) Shape parameter (T) equal to $2(\ln K_2n - \ln K_3m)/(\ln K_1m - \ln K_3m)$ using methods from Jelinek (1981), Ellwood and Crick (1988) and Tarling and Hrouda (1993).

The result is graphically presented, showing the orientation of the three principal axes, $K_1 \geq K_2 \geq K_3$ (maximum, intermediate, and minimum AMS axes, respectively), which are generally referred to as the eigenvectors of the susceptibility tensor. The K_3 axis is perpendicular to foliation and is regarded as the magmatic foliation plane in magmatic rocks, and as the flattening plane in solid-state deformed rocks. K_1 is parallel to the petrofabric lineation, which is often regarded as tectonic lineation and/or magmatic flow direction.

Nine (9) samples were collected from the plutons, and the acquired data were processed using the Anisoft software (Table 1). The data were categorized into scalar (magnitude) and vector (directional) magnetic data.

Table 1. Calculated AMS parameters of samples of Gwandara

SN	K1			K2			K3			K_m ($\times 10^{-3}$) SI	L	F	P%	T
	($\times 10^{-3}$) SI	Dec	Inc	($\times 10^{-3}$) SI	Dec	Inc	($\times 10^{-3}$) SI	Dec	Inc					
G05	0.49	9.499	6.5	0.46	120.93	72.68	0.42	277.63	15.98	0.45	156.80	17.97	16.6	0.1
G07	0.47	9.499	2.1	0.46	101.48	43.42	0.42	277.28	46.50	0.45	771.43	18.75	11.9	0.6
G02	0.18	6.599	12.5	0.16	210.62	76.35	0.15	97.79	5.37	0.39	51.39	48.93	20.1	-0.3
G03	0.78	24.399	27.8	0.61	149.86	47.73	0.49	277.42	28.98	0.62	24.13	11.29	58.1	-0.2
G09	0.69	26.899	4.5	0.66	117.76	10.86	0.52	274.73	78.21	0.62	33.01	12.77	32.6	0.6
G11	0.81	1.399	12.5	0.72	249.83	58.90	0.71	98.15	27.96	0.74	32.78	10.88	15.4	-0.8
G01	0.46	38.799	84.1	0.25	187.47	5.044	0.18	277.74	3.051	0.29	17.80	19.15	155.5	-0.5
G08	0.93	36.7	38.8	0.67	161.61	35.44	0.49	277.34	31.37	0.69	19.42	9.47	89.8	-0.2
G06	1.15	32.299	22.3	0.94	139.08	35.14	0.71	276.78	46.40	0.93	24.96	7.65	61.9	0.1

7.1. Scalar (Magnitude) Magnetic Data

This category of data includes susceptibility magnitudes (K_m) of the samples collected, and this varies between $0.39 - 0.93 \times 10^{-3}$ SI. These sets of bulk susceptibility have been reported to reflect paramagnetic behavior, which is mostly typical of phyllosilicates (Dunlop et al., 2006). Though this range exceeds the generally reported susceptibility value for iron-rich silicate, particularly biotite, this variation, though

insignificant, could mean that other members of the coexisting silicate group, like hornblende, acquired more iron enrichment during iron oxidation. Distribution of magnetic susceptibility across plutons shows that its maximum K_m value was measured at 0.93×10^{-3} SI units (sample no. G06) and the minimum K_m value recorded 0.39×10^{-3} on sample G02. Generally, the marginal variation in the K_m values across the plutons is attributed to the irregularity in the bulk

distributions of responsive minerals in the rock, though ductility in rock, particularly where high fluid flow is enhanced, was argued (Aranguren et al., 1996; Aubourg et al., 1991; Housen et al., 1995).

Other scalar parameters like the Degree of Anisotropy (P%) values range between 11.9% and 89.8% among the pluton and exceptionally 155.5% which suggests that the rock has a strong mineral alignment, thus very strong anisotropy that varies significantly with direction. Bouchez (1997) reported that where the P% values are lower than 15%, it is a magnetite-free rock. This will mean that some samples contain an exceptional occurrence of magnetite. The shape parameter (T) of the AMS ellipsoid shows that 4 of 9 samples have prolate shapes ($T < 0$) ellipsoids and 5 of 9 samples show oblate shapes ($T > 0$) ellipsoids.

7.2. Vector (Directional) Magnetic Data

Generally, the K1 axis of the AMS ellipsoid defines magnetic lineation, and the normal to K3 defines the magnetic foliation. Bouchez (2000) reported that in granite whose magnetism is paramagnetic, the K3 denotes the pole of the foliation, and K1 denotes the lineation, which is characteristic of the rotational axis of foliation of the casualty mineral grains, which in this case is the biotite. The AMS data shows a consistent magnetic fabric across the outcrops (Fig. 9a). The K3 (blue color circle) displays a uniform subhorizontal but mostly WNW alignment. The K1 (magnetic lineation) shows orientations that are almost orthogonal to the K3. It has NNE–SSW to NE–SW. These trends also tally with the general orientation of the outcrop as well as the mineral lineation, with an average of 020°. The shapes of the AMS ellipsoid for five samples were plotted in the oblate while four were plotted in the prolate field (Fig. 9b). This situation depicts a protracted magmatism under a tectonic condition that changes over time, where extensional and strike-slip forces interact, typical of a transtensional zone.

8. Discussion

8.1. Implication of Strain and AMS on the Magmatic Fabrics

The natural state of magmatic fabric is largely incompetent to retain deformation records within magma, apparently occasioned mostly by its weak development in melts and susceptibility to resetting due to non-uniform flow patterns (Paterson et al., 1998).

Consequently, the strain measurements obtained from rock fabrics serve as a chronological record of the incremental deformation experienced by the rock before its complete emplacement. To further substantiate this, a comparative analysis was conducted between the strain measurements of rock fabrics and those of enclaves and xenoliths. This revealed a remarkable uniformity in the trends of generated ellipsoids but contrasted magnitudes as recorded in the axial ratio of the ellipsoids. This observation suggests that the strain recorded in the rocks was influenced by a similar directionally wobbled stress regime.

Similarly, the Anisotropy of Magnetic Susceptibility (AMS) technique revealed the same preferred orientation of rock fabric in response to external forces. The results obtained from this analysis show paramagnetism, which generally is

reflective of a preferred crystallographic orientation of the constituents of the rock. This relationship confirms that there was homogeneity between the magmatic flow pattern and the externally exerted mechanical influence on the pluton.

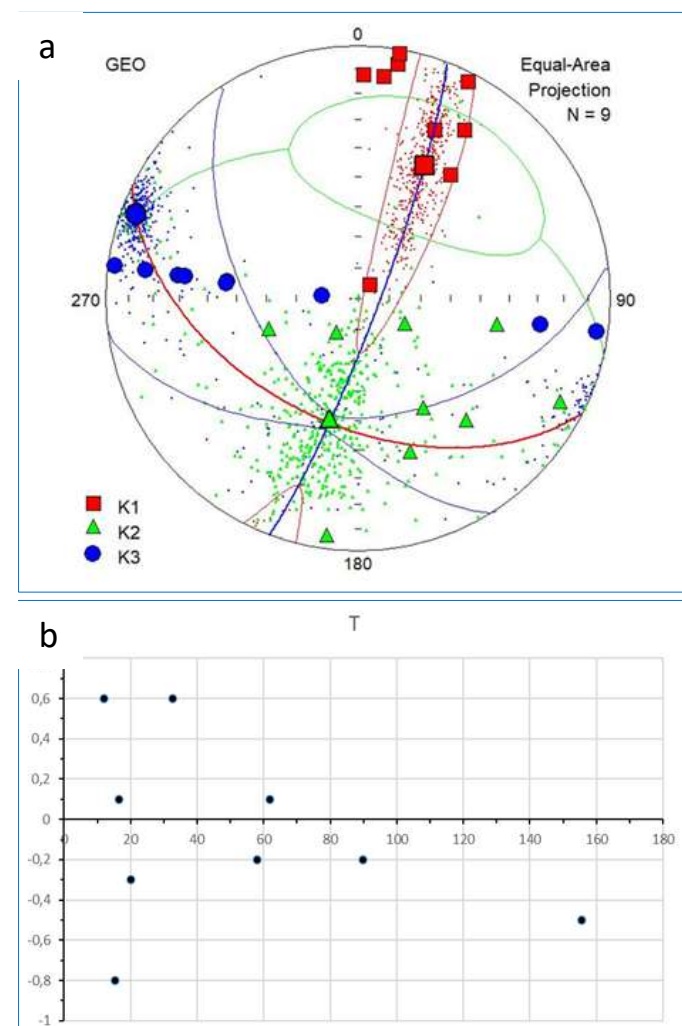


Fig. 9. a) Plot of directional AMS data on Gwandara plutons and b) Plot of shape parameter (T)

Also, the pluton exhibits evidence of sinking stopped blocks. Interestingly, there are no display records of contrasted trends of strain ellipsoids; instead, it exhibited strained ellipsoidal trends remarkably similar to the field-mapped structures. A comprehensive strain analysis of xenoliths and enclaves revealed that these components experienced higher strain levels compared to the surrounding fabric. This discrepancy is attributed to the occurrence of these aggregates above the flow viscosity of the fluid stage, rendering them more competent to record stress activities around the pluton than the fluid itself. Despite this, both categories of ellipsoids exhibit similar trends of maximum stretch, implying that the strain recorded by magmatic fabrics occurred during the regional deformational cycle immediately preceding the total crystallization of the plutons.

8.2. Emplacement Conditions of the Granitic Pluton

It is generally difficult to isolate a single emplacement scenario for this pluton, because both the magma-induced

stress field and the regional crustal dynamics show indications of an active regional tectonic setting. Nevertheless, inferences were drawn from the pluton and host rocks' interactions and microstructural characteristics to infer the possible prevailing rheology conditions. Therefore, the insights offered here are derived from field observations and the petrophysical properties of the rocks.

While the central focus is on the emplacement rather than other aspects of pluton development, the non-consideration of isotopic data limits information on the sources of the magma. However, the significant concentration of silica (>60%) in the rock points to a melt that has crustal involvement in its generation, and the protolithic crust was calc-alkaline rich (Chappell and Stephens, 1988; Roberts and Spencer, 2015) though the occurrence of patches of shredded mafic schlieren layers in the pluton suggest a melt that is contaminated with mantle materials. This may explain the hornblende stains on the pluton.

The rheological conditions that influenced the emplacement of this pluton indicate shallow depth of emplacement controlled primarily by a set of dominantly NE-SW-oriented structures and remnants of reactivated marginal NNW-SSE and N-S structures. The culmination of these structures has further weakened the already polydeformed older basement rocks, thus providing permeable pathways for upward magmatic intrusion. The magma flowed in a manner that overrode, covered, and melted the fragmented walls of the pervasive fractures, embedding the host rock and facilitating further upward propagation, suggesting that the process was predominantly compressive and assimilative in nature. This scenario occurred under a relatively stable regional crustal condition, where only the magmatic-generated stress field was active.

The growth process was limited at the upper level by the interaction between the rising magma and the cooler crust, resulting in increased viscosity, which later impeded further ascent. Meanwhile, as the effectiveness of the magma stress field decreased due to viscosity contrast, further deep-cut fractures developed along the cleavages of the dipping blocks in the southern portion of the emerging pluton. These developed fractures acted as conduits where heat was lost, initiating further increases in viscosity, thereby creating conditions for crystallization at the upper part of the pluton.

Although crystallization began around the upper portion of the pluton due to increased viscosity and heat loss, the magmatic source still maintained a sufficient thermal budget that allowed continuous magma influx into the emplacement chamber. However, this was insufficient to drive further upward ascent, and the impeded ascent created magma-inflated hotspots. These hotspots eventually led to the formation of numerous offshoots around the pluton and caused minor folding episodes in the host rock. Towards the end of the emplacement and its associated activities, there was evidence of a resumed NE-SW transient tectonic reaction dominated by a strike-slip system around the pluton. This led to the development of constrained minor shear zones and realignment of porphyries and mineral grains, particularly in the lower portion of the pluton.

The shape of the pluton appears to have been influenced by a vertical feeder located predominantly below the pluton, in the zone of its maximum curvature. The magma ascended vertically and spread along major poly-fractured planes (as indicated by the consistency in the values and orientation of K1 principal axes), giving the pluton its laccolithic appearance. This suggests that the primary space for emplacement was created by the inherited fracture system from earlier extensional regional tectonics. While there are scenarios at the emplacement site that align with both Ramsay (1981) and Brun and Pons (1981) perspectives on granitic pluton emplacement, the Gwandara pluton's emplacement demonstrates that magma buoyancy, which defined the upward ascent and chamber inflation, were insufficient to create the required space for pluton emplacement at shallow crustal levels, particularly in an active crustal region. Although buoyancy and chamber inflation had a significant impact, the predominant factor was the pre- and syn-sinistral strike-slip tectonic activities.

9. Conclusions

The emplacement of the Gwandara pluton was a complex process influenced largely by a combination of pre-existing fractures, active regional tectonic activities, and a marginal magma-induced stress field. The formation of the pluton was molded by compressive and assimilative processes, with magma rising through permeable pathways created by multiple older tectonic activities. The interaction between magmatically generated stress fields, crustal dynamics, and tectonic reactions shaped the pluton's laccolithic structure and determined its shallow depth of emplacement.

Acknowledgment

We would like to express our gratitude to the staff and management of the Department of Geology and Mining at Nasarawa State University, Keffi, for their support in allowing us to use the departmental laboratory. We particularly appreciate staff for their exceptional encouragement and constructive feedback at every stage of this research.

Conflict of Interest Statement

We hereby certify that there are no affiliations or involvement with any organizations that have any financial interest, in any form, in this study or the materials referenced in this manuscript.

Reference

- Agbo, P., Goki, N.G., Tanko, I.Y., 2025. Assessment of deformation patterns on Pan-African basement rocks of Keffi area (Sheet 208NE), Central Nigeria. *Iconic Research and Engineering Journals* 8 (2), 1076-1085.
- Ajibade, A.C., Rahaman, M.A., Woakes, M., 1987. Proterozoic Crustal Deformation in the Pan-African Regime of Nigeria. In Kogbe, C.A. (ed) *Geology of Nigeria*. Elizabeth Publisher, Lagos pp. 57-69.
- Aranguren, A., Cuevas, J., Tubia, J.M., 1996. Composite magnetic fabrics from S-C mylonites. *Journal of Structural Geology* 18 (7), 863-869. [https://doi.org/10.1016/0191-8141\(96\)00013-2](https://doi.org/10.1016/0191-8141(96)00013-2).
- Aubourg, C., Rochette, P., Vialon, P., 1991. Subtle stretching lineation revealed by magnetic fabric of Callovian –Oxfordian black shales (French Alps). *Tectonophysics* 185, 211-223.

Barker, A.J., 1998. Introduction to Metamorphic textures and Microstructures (2nd Ed.) Stanley Thornes (Publishers) Ltd. United Kingdom. 508 pp.

Black, R., Latouche, L., Liegeois, J.P., Caby, R., Bertrand, J.M., 1994. Pan-African displaced terranes in the Tuareg shield (central Sahara). *Geology* 22, 641-644.

Borradaile, G.J., Henry, B., 1997. Tectonic applications of magnetic susceptibility and its anisotropy. *Earth-Science Reviews* 4, 49-93.

Bouchez, J.L., 2000. Anisotropie de susceptibilité magnétique et fabrique des granites. *Comptes-Rendus à l'Académie des Sciences de Paris* 330, 1-14.

Bouchez, J.L., 1997. Granite is never isotropic: an introduction to AMS studies of granitic rocks. In: Bouchez, J.L., Hutton, D., Stephens, W.E. (Eds.), *Granite: from Segregation of Melt to Emplacement Fabrics*, Kluwer, Dordrecht, pp. 95-111.

Brun, J.P., Pons, J., 1981. Strain patterns of pluton emplacement in a crust undergoing non-coaxial deformation: *Journal of Structural Geology* 3, 219-229.

Caby, R., 1989. Precambrian terranes of Benin-Nigeria and Northeast Brazil and the Late Proterozoic South Atlantic fit. In: DALLMEYER, R. D. (ed.) *Terranes in the Circum-Atlantic Paleozoic Orogens*. Geological Society America, Special Papers, 230, 145-158.

Chappell, B.W., Stephens, W.E., 1988. Origin of infracrustal I-type granite magmas. *Transactions of the Royal Society of Edinburgh (Earth Sciences)* 79, 71-86.

Dada, S.S., Tubosun, I.A., Lancelot, J.R., Lar, A.U., 1993. Late Achaean U-Pb age for the reactivated basement of Northeastern Nigeria. *Journal of African Earth Sciences* 16, 405-412.

Dada, S.S., Briqueu, L., Harms, U., Lancelot, J.R., Mattheis, G., 1995. Charnockitic and monzonitic Pan-African series from north central Nigeria: Trace-element and Nd, Sr, Pb isotope constraints on their petrogenesis. *Chemical Geology (Isotope Geoscience)* 124, 233–252.

Dada, S.S., Lancelot, J.R., Briqueu, L., 1989. Age and origin of the annular charnockitic complex at Toro, Northern Nigeria: U-Pb and Rb-Sr evidence. *Journal of African Earth Sciences* 9, 227-234.

Dunlop, D.J., Ozdemir, O., Rancourt, D.G., 2006. Magnetism of biotite crystals. *Earth and Planetary Science Letters* 243 (3-4), 805-819.

Egbuniwe, I.G., Fitches, W.R., Bentley, M., Snelling, N.J., 1983. Late Pan African syenite-granite plutons in NW Nigeria. *Journal of African Earth Sciences* 3 (4), 427-435.

Ellwood, B.B., Crick, E.C., 1988. Paleomagnetism of Paleozoic asphalt deposits in southern Oklahoma, USA. *Geophysical Research Letters* 15 (5), 436-439.

Evans, M.A., Lewchuk, M.T., Elmore, R.D., 2003. Strain partitioning of deformation mechanism in limestones: Examining the relationship of strain and anisotropy of magnetic susceptibility (AMS). *Journal of Structural Geology* 25 (9), 1525-1549. [https://doi.org/10.1016/S0191-8141\(02\)00186-4](https://doi.org/10.1016/S0191-8141(02)00186-4)

Ferre', E.C., Gleizes, G., Caby, R., 2002. Obliquely convergent tectonics and granite emplacement in the Trans-Saharan belt of Eastern Nigeria: a synthesis. *Precambrian Research* 114, 199-219.

Gapais, D., 1989. Shear structures within deformed granites: Mechanical and thermal indicators. *Geology* 17, 1144-1147.

Goki, N.G., Umbugadu, A.A., 2022. Structural evolution and geomorphological terrane influence on groundwater seepage in the Maloney Ridge Kef, Central Nigeria. *Arabian Journal of Geosciences* 15, 1197. <https://doi.org/10.1007/s12517-022-10437-3>.

Goki, N.G., Abba, S.I., 2019. Geochemistry of I-type Granites from the Area Around Gwagwada, Kaduna, Nigeria. *Online Journal of Earth Sciences* 13 (2), 15-25.

Handy, M.R., 1990. The solid state flow of polymimetic rock. *Journal of Geophysical Research* 95 (B6), 8647-8661.

Haruna, I.V., 2014. Petrology and Geochemistry of Granitoids of the Northern Part of Adamawa Massif, N.E Nigeria. *Journal of Geology & Geophysics* 3 (6), 177. <https://doi.org/10.4172/2329-6755.1000177>.

Housen, B.A., van der Pluijm, B.A., Essene, E.J., 1995. Plastic behaviour of magnetite and high strains obtained from magnetic fabrics in the Parry Sound shear zone, Ontario, Grenville Province. *Journal of Structural Geology* 17, 265-278.

Jelinek V., 1981. Characterization of the magnetic fabric of the rock. *Tectonophysics* 79, 563-567.

Paterson, S., Fowler, T., Schmidt, K., Yoshinobu, A., Yuan, E., Miller, R., 1998. Interpreting magmatic fabric patterns in plutons. *Lithos* 44, 53-82.

Pidgeon, R.T., 1976. Pan-African and earlier events in the basement complex of Nigeria [abs.]: Sydney, International Geological Congress 3, 667.

Rahaman, M.A., 1988. Recent Advances in the study of the Basement Complex of Nigeria. In *Geological Survey of Nigeria* (Ed), *Precambrian Geology of Nigeria* pp. 11-41.

Ramsay, J.G., 1981. Emplacement mechanics of the Chindamora Batholith, Zimbabwe (abstract). In: *Diapirism and Gravity Tectonics: Report of a Tectonic Studies Group* (edited by Coward, M. P.). *Journal of Structural Geology* 3, 89-95.

Tarling, D.H., Hrouda, F., 1993. The magnetic anisotropy of rocks. Chapman & Hall, London 217 pp.

Truswell, J.F., Cope, R.N., 1963. The geology of parts of Niger and Zaria provinces, Northern Nigeria. *Bulletin No. 29*. Published by Geological Survey of Nigeria. Pp.17-22.

Ugwuonah, E.N., Tsunogae, T., Obiora, S.C., 2017. Metamorphic P-T evolution of garnet-staurolite-biotite pelitic schist and amphibolite from Kef, North-Central Nigeria: Geothermobarometry, Mineral Equilibrium Modeling and P-T Path. *Journal of African Earth Sciences* 129, 1-16.

Ugwuonah, E.N., Obiora, S.C., 2011. Geothermometric and Geobarometric Signatures of Metamorphism in the Precambrian Basement Complex Rocks Around Keffi, North-Central Nigeria. *Ghana Journal Science* 51, 73-87.